

Supplementary Materials

The Influence of the Electrodeposition Parameters on the Properties of Mn-Co-Based Nanofilms as Anode Materials for Alkaline Electrolyzers

Karolina Cysewska ^{1,*}, Maria Krystyna Rybarczyk ², Grzegorz Cempura ³, Jakub Karczewski ⁴, Marcin Łapiński ⁴, Piotr Jasinski ¹ and Sebastian Molin ¹

¹ Faculty of Electronics, Telecommunications and Informatics, Gdańsk University of Technology, ul. Narutowicza 11/12, 80-233 Gdańsk, Poland; piotr.jasinski@pg.edu.pl (P.J.); sebastian.molin@pg.edu.pl (S.M.)

² Chemical Faculty, Department of Process Engineering and Chemical Technology, Gdańsk University of Technology, ul. Narutowicza 11/12, 80-233 Gdańsk, Poland; maria.rybarczyk@pg.edu.pl

³ Faculty of Metals Engineering and Industrial Computer Science, International Centre of Electron Microscopy for Materials Science, AGH University of Science and Technology, ul. A. Mickiewicza 30, 30-059 Krakow, Poland; cempura@agh.edu.pl

⁴ Faculty of Applied Physics and Mathematics, Gdańsk University of Technology, ul. Narutowicza 11/12, 80-233 Gdańsk, Poland; jakkarcz@pg.edu.pl (J.K.); marcin.lapinski@pg.edu.pl (M.Ł.)

* Correspondence: karolina.cysewska@pg.edu.pl

Received: 21 May 2020; Accepted: 10 June 2020; Published: 11 June 2020

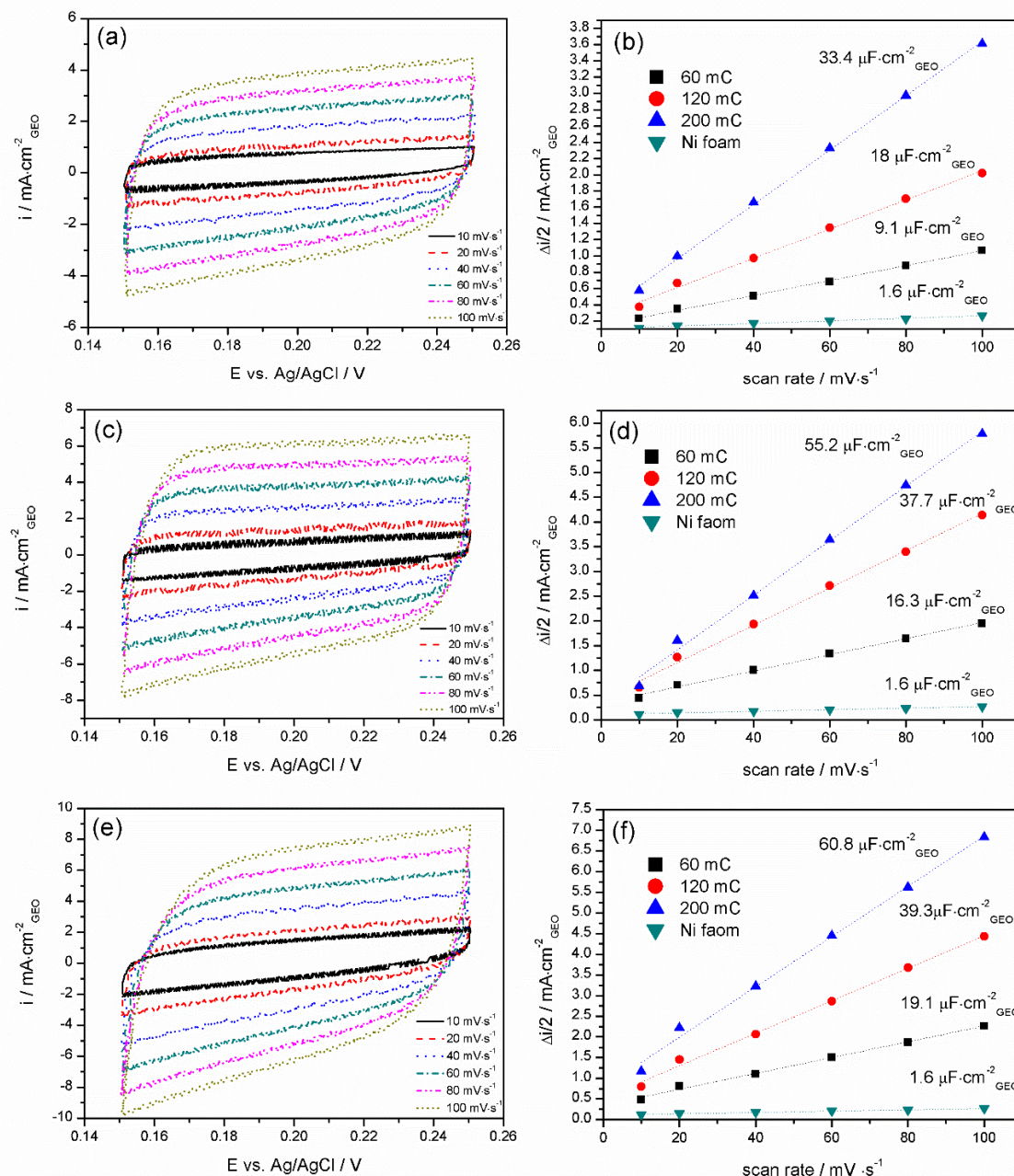


Figure S1. Cyclic voltammograms recorded during sweeping the potential from 0.15 to 0.25 V vs. Ag/AgCl with different scan rates in aqueous solution of 1 M KOH for Mn-Co film synthesized in solution of Mn:Co 2:4 mM (a), 2:6 mM (c) and 2:8 mM (e) for 200 mC. Corresponding linear approximation of the capacitive currents versus scan rate obtained from cyclic voltammograms for Mn-Co film synthesized in solution of Mn:Co 2:4 mM (b), 2:6 mM (d) and 2:8 mM (f) for different deposition charge.

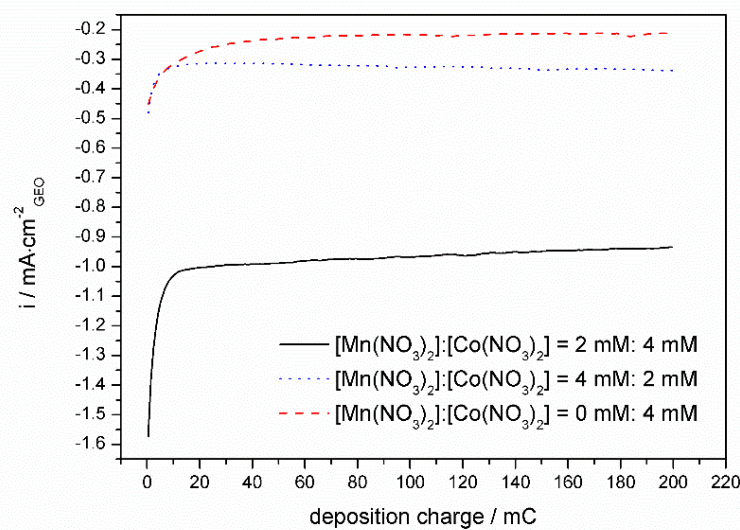


Figure S2. Synthesis graphs recorded during the potentiostatic deposition of Mn/Co oxide/hydroxides at -1.1 V vs. Ag/AgCl in aqueous solution of differently concentrated $\text{Mn}(\text{NO}_3)_2 \cdot 4\text{H}_2\text{O}$ and $\text{Co}(\text{NO}_3)_2 \cdot 6\text{H}_2\text{O}$ with electropolymerization time limited by a charge of 200 mC .

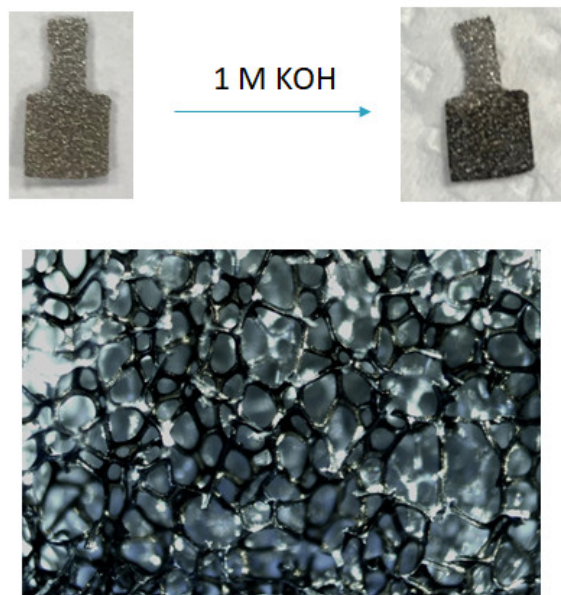


Figure S3. Optical microscopy image of the as-deposited and after alkaline treatment in 1 M KOH Mn-Co film on nickel foam.

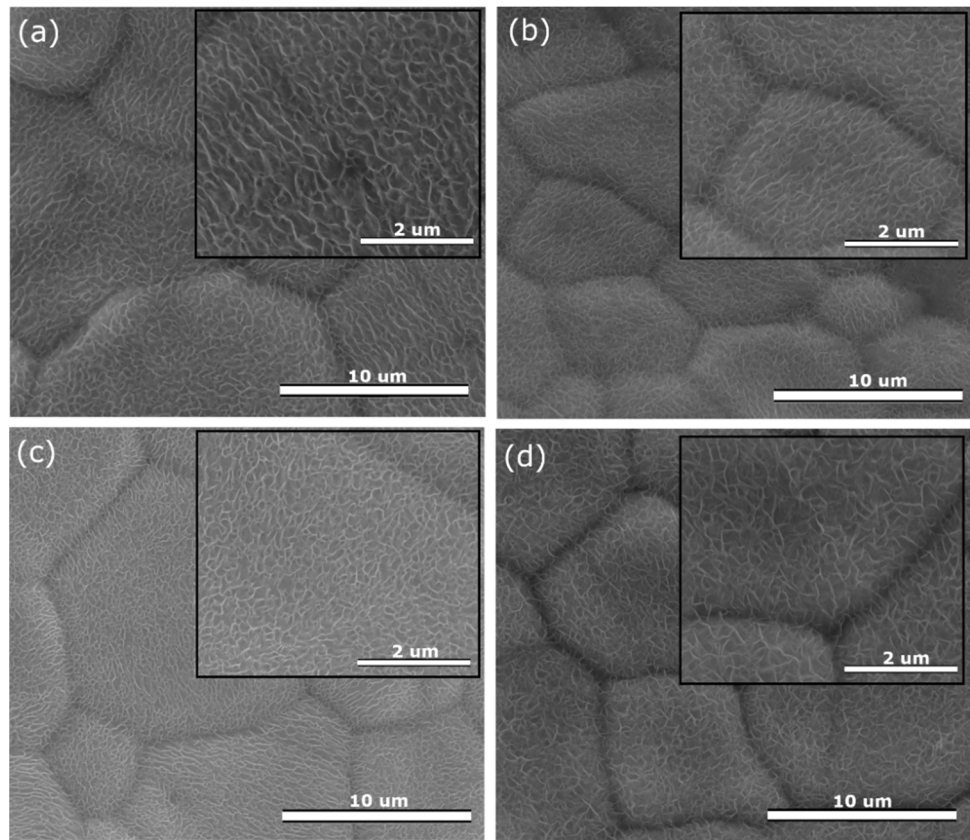


Figure S4. SEM images of Mn-Co film synthesized in aqueous solution of Mn:Co 2:4 mM for 60 mC (a), 2:4 mM for 120 mC (b), 2:4 mM 200 mC (c) and 2:6 mM 200 mC (d) on nickel foam.

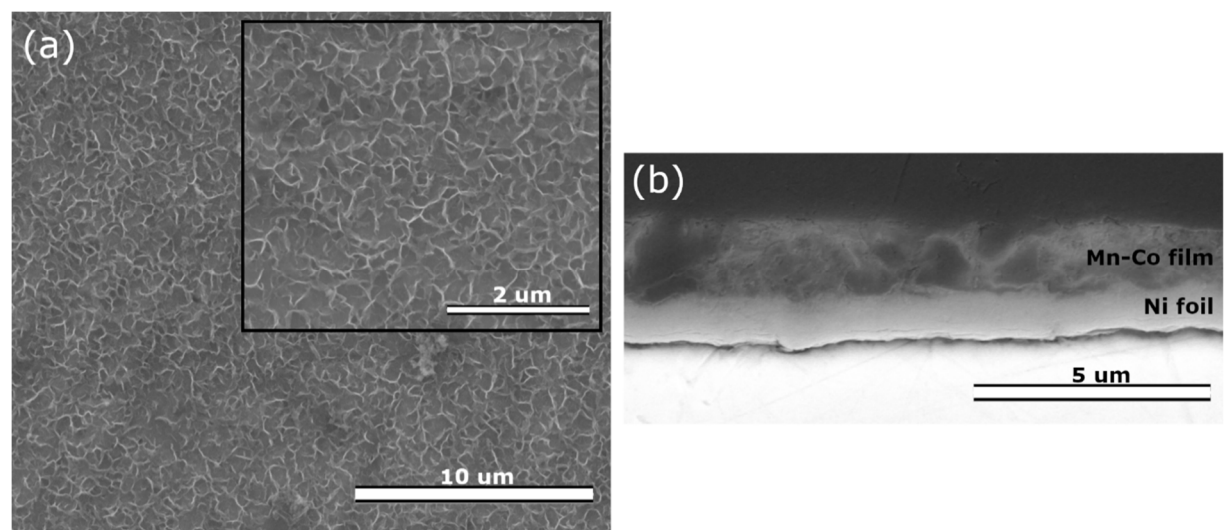


Figure S5. SEM images of Mn-Co film synthesized in aqueous solution of Mn:Co 2:4 mM for 60 mC (a) and 2:8 mM for 200 mC (b) on nickel foil.

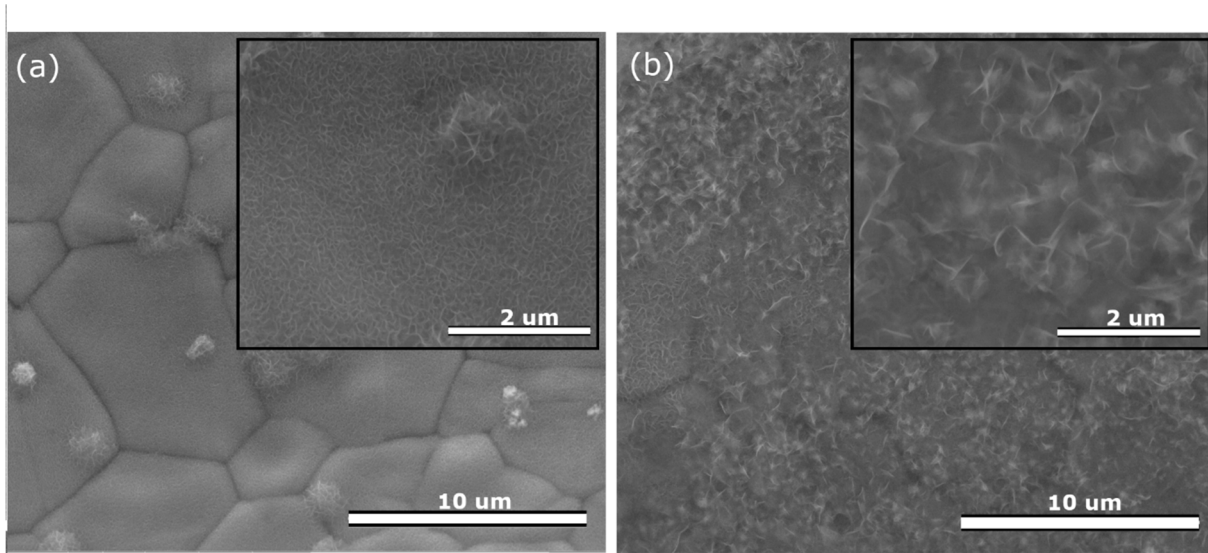


Figure S6. SEM images of Mn-Co film synthesized in aqueous solution of (a) 4 mM $\text{Co}(\text{NO}_3)_2 \cdot 6\text{H}_2\text{O}$ or (b) 4 mM $\text{Mn}(\text{NO}_3)_2 \cdot 4\text{H}_2\text{O}$ and 2 mM $\text{Co}(\text{NO}_3)_2 \cdot 6\text{H}_2\text{O}$ on nickel foam for 200 mC

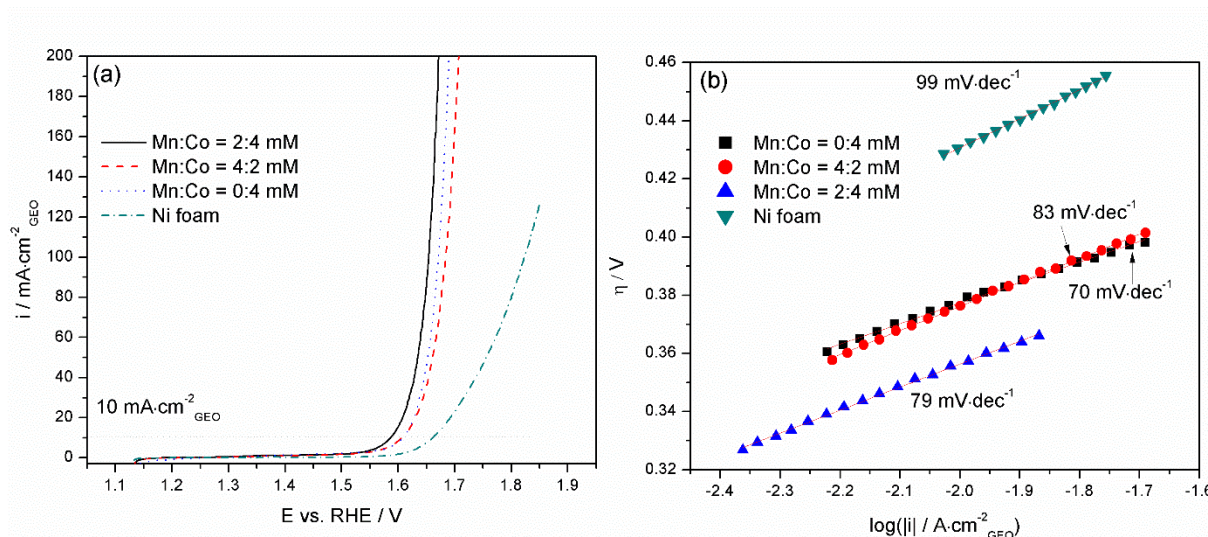


Figure S7. Linear sweep voltammetry profiles (a) and corresponding Tafel plots (b) of Mn-Co film synthesized in solution of Mn:Co 2:4 mM, 4:2 mM and 0:4 mM on nickel foam measured in Ar-purged 1 M KOH. .

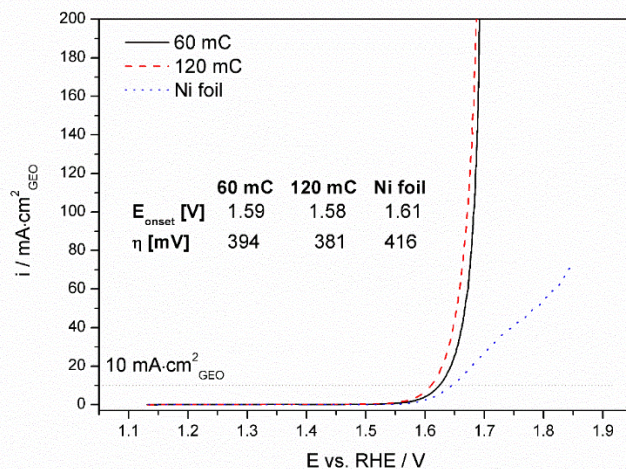


Figure S8. Linear sweep voltammetry profiles of nickel foil and Mn-Co film synthesized in solution of Mn:Co 2:8 mM for 60 and 120 mC on nickel foil.

Table S1. Comparison of catalyst based on Mn and/or Co transition metals synthesized electrochemically for OER activity available in the literature.

catalyst	substrate	solution	$E_{\text{onset}} / \text{V vs. RHE}$	$\eta (10 \text{ mA} \cdot \text{cm}^{-2} \text{geo}) / \text{mV}$	Ref.
Mn-Co	Ni foam	1 M KOH	1.47	335	This work
CoMn-LDH	carbon	0.1 M KOH	-	258	[1]
MnO ₂	carbon	0.1 M KOH	-	424	[1]
MnO _x -573K	F:SnO ₂	1 M KOH	-	570 at 20 mA·cm ⁻² geo	[2]
Mn ₃ O ₄	F:SnO ₂	1 M KOH	-	570	[2]
Co ₃ O ₄	Ni foil	0.1 M KOH	1.58	530	[3]
Co ₃ O ₄	SS	1 M KOH	-	603 at 100 mA·cm ⁻² geo	[4]
Co ₃ O ₄	Pt	1 M KOH	-	410	[5]
Ni _{0.6} Co _{2.4} O ₄	Ni foil	0.1 M KOH	1.57	-	[3]
Zn _x Co _{3-x} O ₄	Au	1 M NaOH	-	330	[6]
ZnCo ₂ O ₄	Ni foam	1 M KOH	-	390	[5]

References

- Yan, F.; Guo, D.; Kang, J.; Liu, L.; Zhu, C.; Gao, P.; Zhang, X.; Chen, Y. Fast fabrication of ultrathin CoMn LDH nanoarray as flexible electrode for water oxidation. *Electrochim. Acta* **2018**, *283*, 755–763.
- Ramírez, A.; Hillebrand, P.; Stellmach, D.; May, M.M.; Bogdanoff, P.; Fiechter, S. Evaluation of MnO_x, Mn₂O₃, and Mn₃O₄ electrodeposited films for the oxygen evolution reaction of water. *J. Phys. Chem. C* **2014**, *118*, 14073–14081.
- Lambert, T.N.; Vigil, J.A.; White, S.E.; Davis, D.J.; Limmer, S.J.; Burton, P.D.; Coker, E.N.; Beechem, T.E.; Brumbach, M.T. Electrodeposited Ni_xCo_{3-x}O₄ nanostructured films as bifunctional oxygen electrocatalysts. *Chem. Commun.* **2015**, *51*, 9511–9514.
- Wu, L.K.; Hu, J.M. A silica co-electrodeposition route to nanoporous Co₃O₄ film electrode for oxygen evolution reaction. *Electrochim. Acta* **2014**, *116*, 158–163.
- Kim, T.W.; Woo, M.A.; Regis, M.; Choi, K.S. Electrochemical synthesis of spinel type ZnCo₂O₄ electrodes for use as oxygen evolution reaction catalysts. *J. Phys. Chem. Lett.* **2014**, *5*, 2370–2374
- Han, S.; Liu, S.; Wang, R.; Liu, X.; Bai, L.; He, Z. One-step electrodeposition of nanocrystalline Zn_xCo_{3-x}O₄ films with high activity and stability for electrocatalytic oxygen evolution. *Acad Appl. Mater. Interfaces* **2017**, *9*, 17186–17194



© 2019 by the authors. Submitted for possible open access publication under the terms and conditions of the Creative Commons Attribution (CC BY) license (<http://creativecommons.org/licenses/by/4.0/>).